PIV/PLIF measurements in non-reacting flow of a GT-burner at realistic flow rates

Chikishev L.M.[1,2*], Lobasov A.S.[1,2], Sharaborin D.K.[1,2], Gobyzov O.A.[1,2], Dulin V.M.[1,2], Bilsky A.V.[1,2], Tsatiashvili V.V.[3], Avgustinovich V.G.[3], Markovich D.M.[1,2]

[1]Novosibirsk State University, Novosibirsk, Russia
[2]Kutateladze Institute of Thermophysics, Novosibirsk, Russia
[3]Combustion chamber department, JSC Aviadvigatel, Perm, Russia
*corresponding author: l.chikishev@gmail.com

Abstract In this work simultaneous velocity field and concentration field measurements at realistic flow-rates conditions (up to 0.5 kg/s air flow and boost pressure) were carried out in a cold flow premixed GT-burner provided by JSC Aviadvigatel. The Reynolds number based on the mean flow rate and nozzle diameter was 300 000. For safety reasons the real fuel (natural gas) was replaced with neon gas to simulate stratification in a strongly swirling flow.
Acetone was seeded into the neon flow to provide quantitative fuel concentration measurements based on planar laser-induced fluorescence (PLIF). Velocity measurements were carried out using particle image velocimetry approach (PIV). The air flow was seeded with water-glycerol mixture particles. This paper reports on details of instantaneous combined measurements of concentration and velocity. It was a challenge to make an accurate measurements due to reflections, absorption and compromise between transparence of the combustion chamber walls and required seeding density. However the quality of experimental data and image processing algorithms allowed to measure simultaneous velocity and passive tracer concentration fields.

Keywords: PIV, acetone PLIF, swirling flow, GT-burner

1 Introduction

Fuel-air mixing plays one of a key roles in flame stabilization and pollutant formation. Computational fluid dynamics code validation, using for complex swirling industrial flows demands on reliable experimental data. In particular, one of the key parameters for computational model verification is turbulent transport of passive admixture. Laser-induced fluorescence of acetone vapor (acetone PLIF) in combination with particle image velocimetry (PIV) can be used for quantitative measurements of local fuel/air ratio at constant temperature and pressure without chemical reaction [1]. There are several advantages of the acetone as a tracer in comparison with other polyatomic molecules: a high vapor pressure at room temperature, an absorption feature accessible with high-pulse-energy lasers, short emission lifetime, low toxicity, low cost for seeding at high flowrates, compatibility with air, insensitivity to effects of collisional quenching, and high fluorescence signal levels. At room temperature and atmospheric pressure acetone had a broadband absorption feature which extends from 225 to 320 nm with a peak near 275 nm. Fluorescence in the wavelength range between 350 and 550 nm is emitted from the first excited singlet state S_1, following laser excitation from the ground electronic state S_0. For example authors of paper [2] investigated turbulent mass-transport for transverse jet flows of laboratory scale. From the other hand PIV/PLIF technique is very robust for measurements at realistic flow-rates. Present paper is focused on flow structure measurements and mass-transfer investigation in premixing GT-burner.

2 Experimental setup

The measurements were carried out in cold combustion chamber model (see Fig. 1). The burner was provided by JSC Aviadvigatel (Perm, Russia). The diameter of the burner was 80 mm. This burner have two channels for fuel supply (in this study fuel was supplied only through the central channel). Main air flow fell into the plenum chamber through four hoses (intake collector). Inside the plenum chamber turbulence generating grid of coaxial form was installed. The coaxial swirler of the burner generated high-swirl premixed flow. The model fuel (neon gas) was supplied to the central channel of the burner. Test section of combustion chamber was made from quartz glass (120 mm inner diameter). An optical section was 170 mm

long.
The maximum air flow-rate was up to 0.5 kg/s. The Reynolds number based on the nozzle diameter, viscosity of the air and the bulk velocity was about 300 000. The pressure inside the chamber was 2 atm with pressure drop at premixer was 4%. For safety reasons neon gas was used instead of methane to model stratification in swirling flow. The gas was supplied from a tank with maximum pressure 10 atm. The neon flowrate was controlled using Bronkhorst flowmeters. The main air flow was supplied from compressed air line. The temperature of the air was 17 °C. Water-glycerol particles were used to provide PIV measurements (the main air flow was seeded). The seeder was connected to the main air pipe (see Fig. 1) via bypass with 0.5 atm pressure difference between inlet and exit of the seeder. The acetone bubbler (the neon flow was seeded) was used to provide PLIF measurements. Neon massflow was 5.4 g/s. The bubbler was temperature stabilized. So at constant flow-rate the acetone vapor concentration in neon flow was constant.

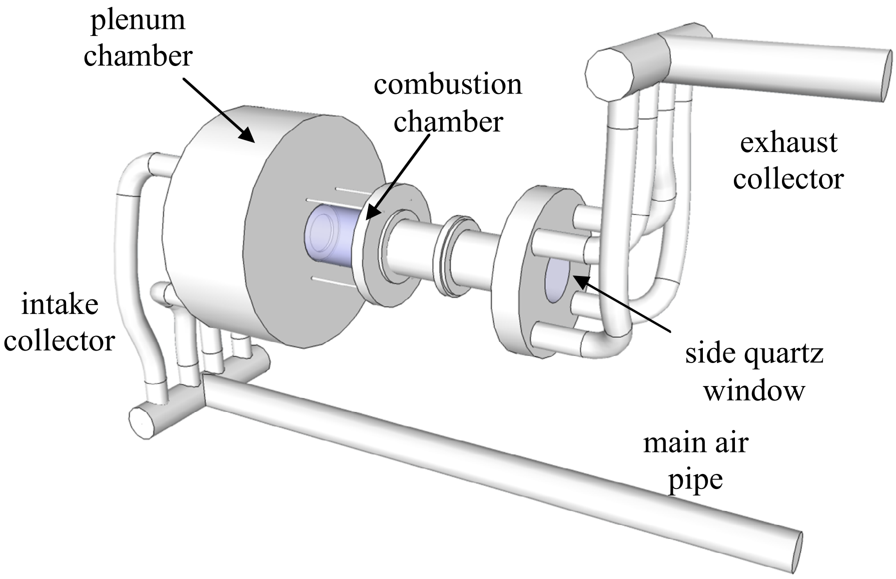

Fig. 1 3D sketch of the experimental setup

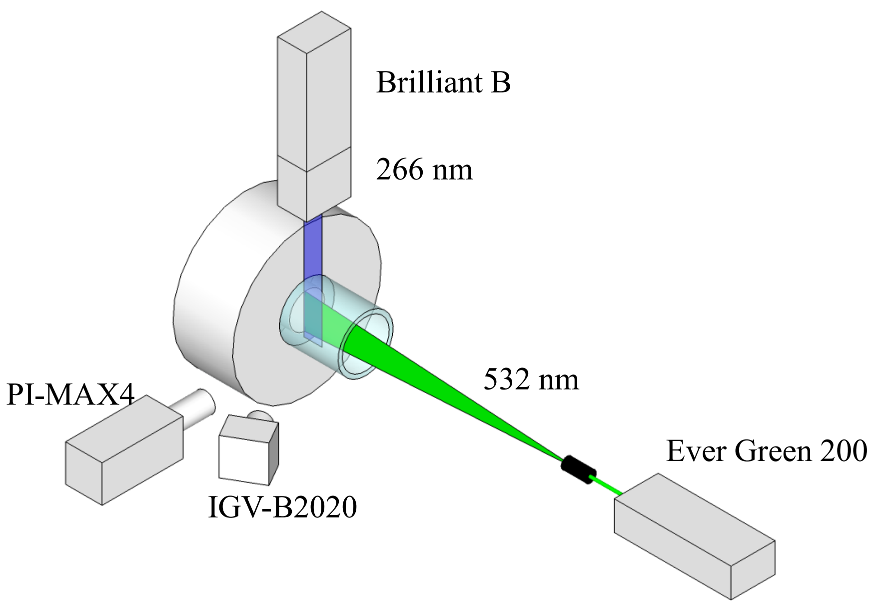

Fig. 2. Scheme of the PIV/PLIF system arrangement

The optical setup for combined PIV/PLIF measurements is depicted in Fig. 2. PIV system consisted of double pulsed Nd:YAG laser (Quantel Ever Green 200) and 4M CCD camera ImperX IGV-B2020. Camera lens SIGMA AF 50 mm (F2,8 EX DG Macro) with optical band-pass filter (Edmund Optics, 532±10 nm, 60% transmittance) was used. To provide laser sheet delivering inside the test section and to minimize scattering and reflections of the beam side quartz window was installed at the end of the cylindrical section. PLIF system included Quantel Brilliant B Nd:YAG laser and ICCD camera PI-MAX-4 (Princeton Instruments). Quantum efficiency of the s20 photocathode in spectral region 290-320 nm is about 25 %. LaVision UV-lens (f#2.8, 100 mm) with interference band-pass optical filter (280-600 nm) and multi-notch filter (1064, 532, 355 nm) was set on the camera. Exposure time of the camera was 200 ns. Fourth harmonic of Nd:YAG laser (266 nm) was used to excite fluorescence of the acetone vapor. Average pulse energy measured with Coherent LabMax Top was 70 mJ. To provide quantitative measurements collimated Sheet Optics (LaVision) was used. This two systems were synchronized using pulse generator (Berkeley Nucleonics BNC 575 TTL). Green laser pulse to pulse delay was 2 mks to prevent particle loss owing to out-of plane velocity component. ICCD camera was exposed between PIV laser pulses.
To make sure that PIV and PLIF area of interest are corresponded a sheet of sensitive paper was placed into the measurement volume and two single shots of 266 and 532 nm lasers were done after each run. This test has shown that measurement regions are well aligned. To measure magnification factor and the mapping functions of two cameras a calibration target was placed inside the cylinder. The distance between markers was 4 mm (see Fig. 3). In several minutes after seeding start the water-glycerol particles formed a film on a chamber wall making the cylinder non-transparent (see Fig. 3c). Thus maximum statistics per one run was about 300 couples of images at 5 Hz frame-rate. The full statistics was 4000 fields of velocity and concentration respectively.

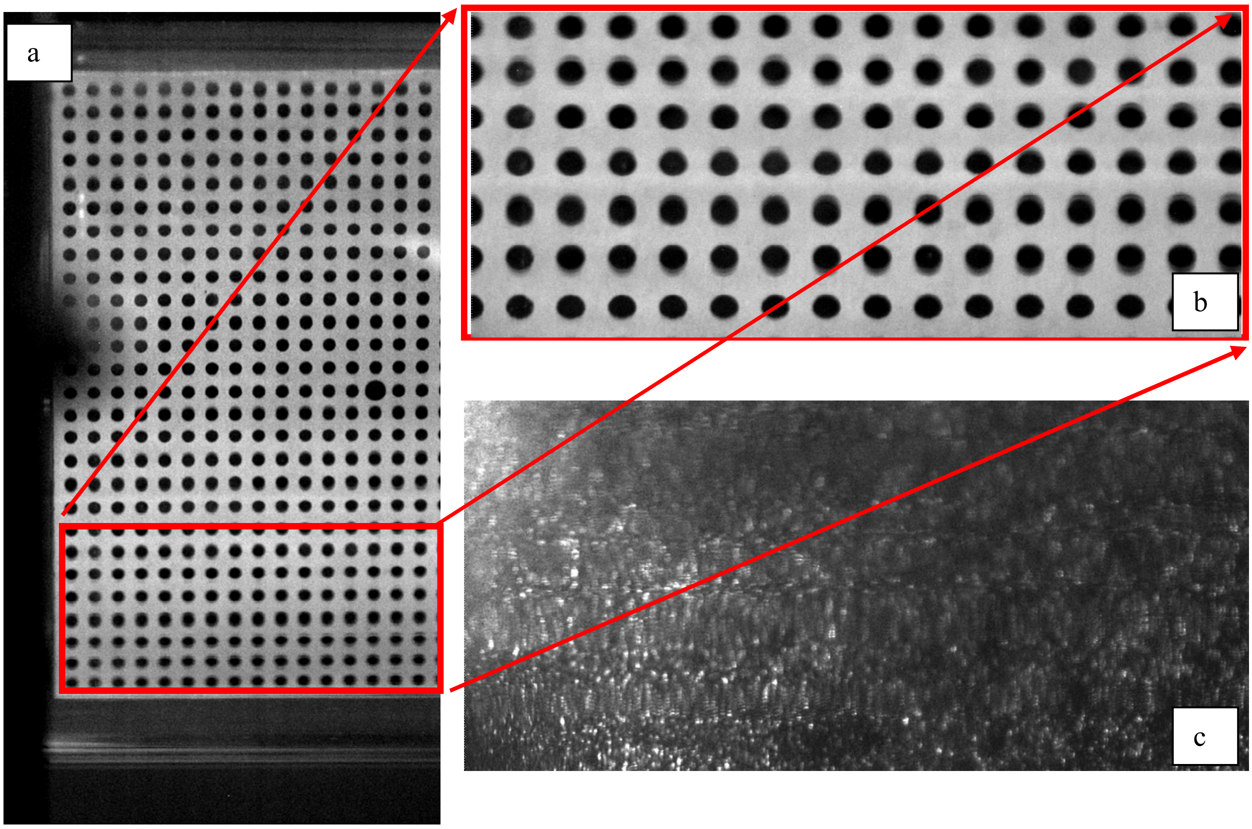

Fig. 3 Calibration target image (a); the influence of the cylinder (b) and particles contamination (c) on the image quality

Data processing

Since PIV camera was inclined to the measurement plane a correction of the perspective distortions was

applied to the PIV images. For calibration of the camera second order polynomial model [3] was used. The PIV data were processed using cross-correlation iterative algorithm with 64x64 interrogation area size was used (the final interrogation size was 32x32 with 75 % overlapping). Peak validation and adaptive median filter (5x5) were used to interpolate false vectors. The spatial resolution was 2 vectors per 1 mm.
As it is known the linear dependency of the fluorescence signal and the acetone tracer concentration is only given if the energy flux in the light sheet is below the saturation level and absorption is neglected. It was previously reported that linear response of acetone vapor at maximum energy flux of 353 mJ/cm^3 when excited at 266 nm (10 ns pulse width) [4]. The maximum laser energy flux in the experiment was 140 mJ/cm^3. The linearity of the signal was verified prior to measurements and no evidence of saturation was found.

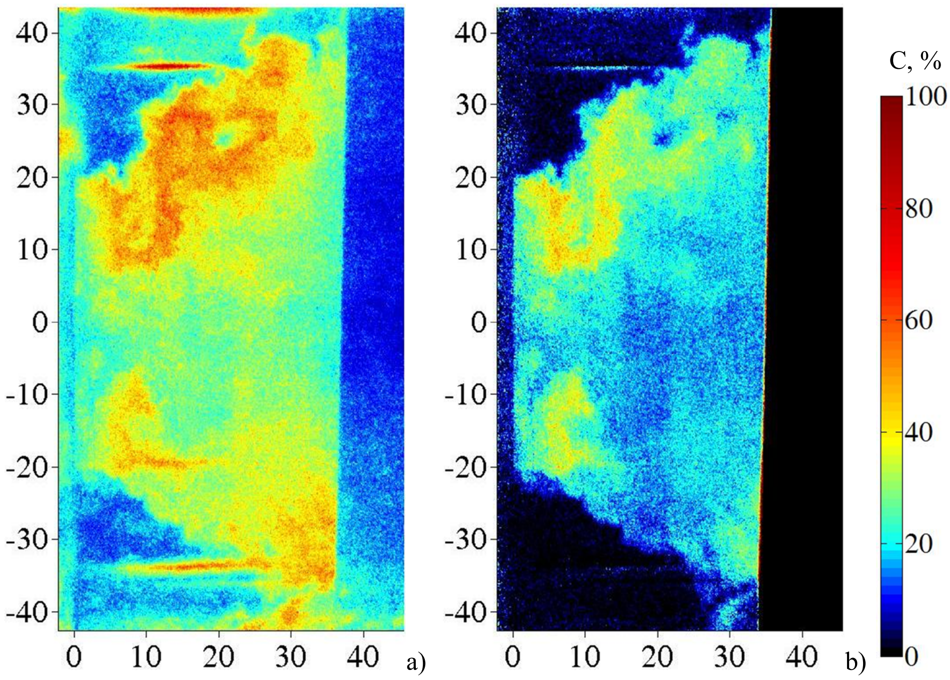

Fig. 4 Instantaneous raw acetone PLIF image (a) and image after all correction procedures (b)

The raw PLIF images were processed using background subtraction and laser sheet correction procedures. After background subtraction images were divided by a sensitivity image. The sensitivity image was recorded while the test section was flooded with an acetone tracer at homogeneous concentration (averaged over 200 images). This procedure accounts for the angular lens collection efficiency, variations of sensitivity of the camera, the quantum efficiency of fluorescence and spatial variations of laser intensity. In order to correct for additional shot-to-shot fluctuations, each single image was corrected according to laser intensity deviation at the same time. Intensity variations were extracted using energy meter. Fig. 4 shows an example of PLIF image evaluation (raw image and image after all correction procedures). The laser sheet direction is from top to bottom. The systematic error was significantly reduced using correction procedures.

Results and discussion

Averaged velocity field is presented in Fig. 5 (red line indicates the backflow region). As could be seen the flow is strongly swirled. After sudden expansion backflow region appears. The maximum velocity at the burner exit is up to 80 m/s. Main feature of the flow is a well pronounced recirculation region extending up to 1D. However the central region of the flow exhibits jet flow due to model fuel supply at the center of the burner (maximum axial velocity 20 m/s). As expected the flow accelerates near wall. The velocity maximum region reaches the wall at approximately 15 mm downstream of the burner. The corner recirculation region is not resolved due to poor signal/noise ratio at the chamber wall caused by laser reflections from the burner. In more details flow structure could be explained using the velocity profiles (Fig. 6). Axial and radial velocity components are presented for two distances downstream of the burner (0,1D and 0,5D respectively).

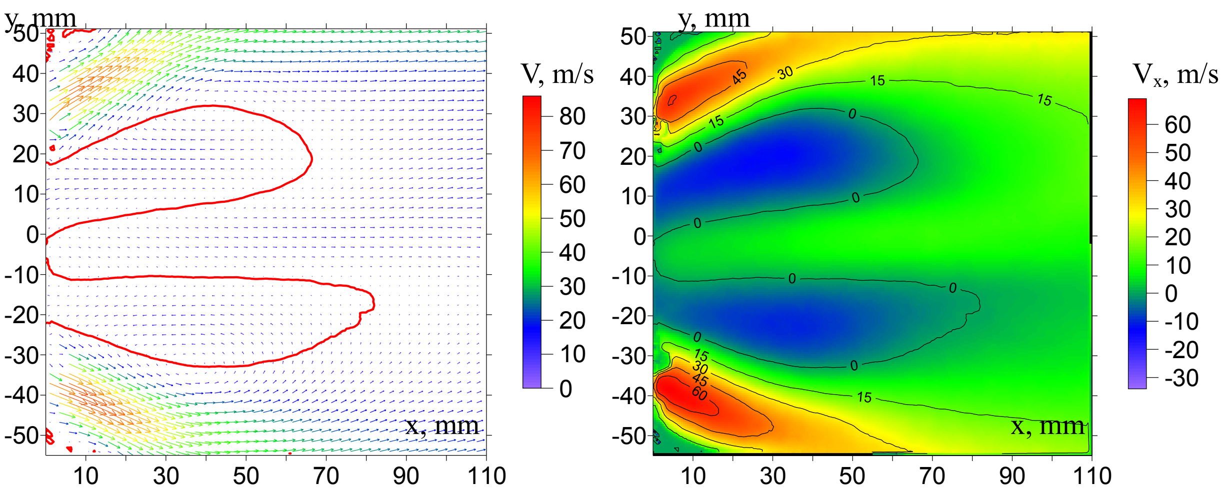

Fig. 5. Averaged velocity field (a) and axial velocity component field (b)

The prominent features of the mean axial velocity profiles are the inflow region with high velocities and pronounced recirculation zone with mean velocities of the order -10 m/s. The RMS values increases slightly with a distance from the axis of symmetry of the burner and have peaks in the inner and outer shear layers. Another feature of the flow is the central jet flow with axial velocity up to 10 m/s. Radial component of the velocity have its maxima only at the initial region of the flow. Downstream the burner mean radial velocity is about zero with RMS about 10 m/s.

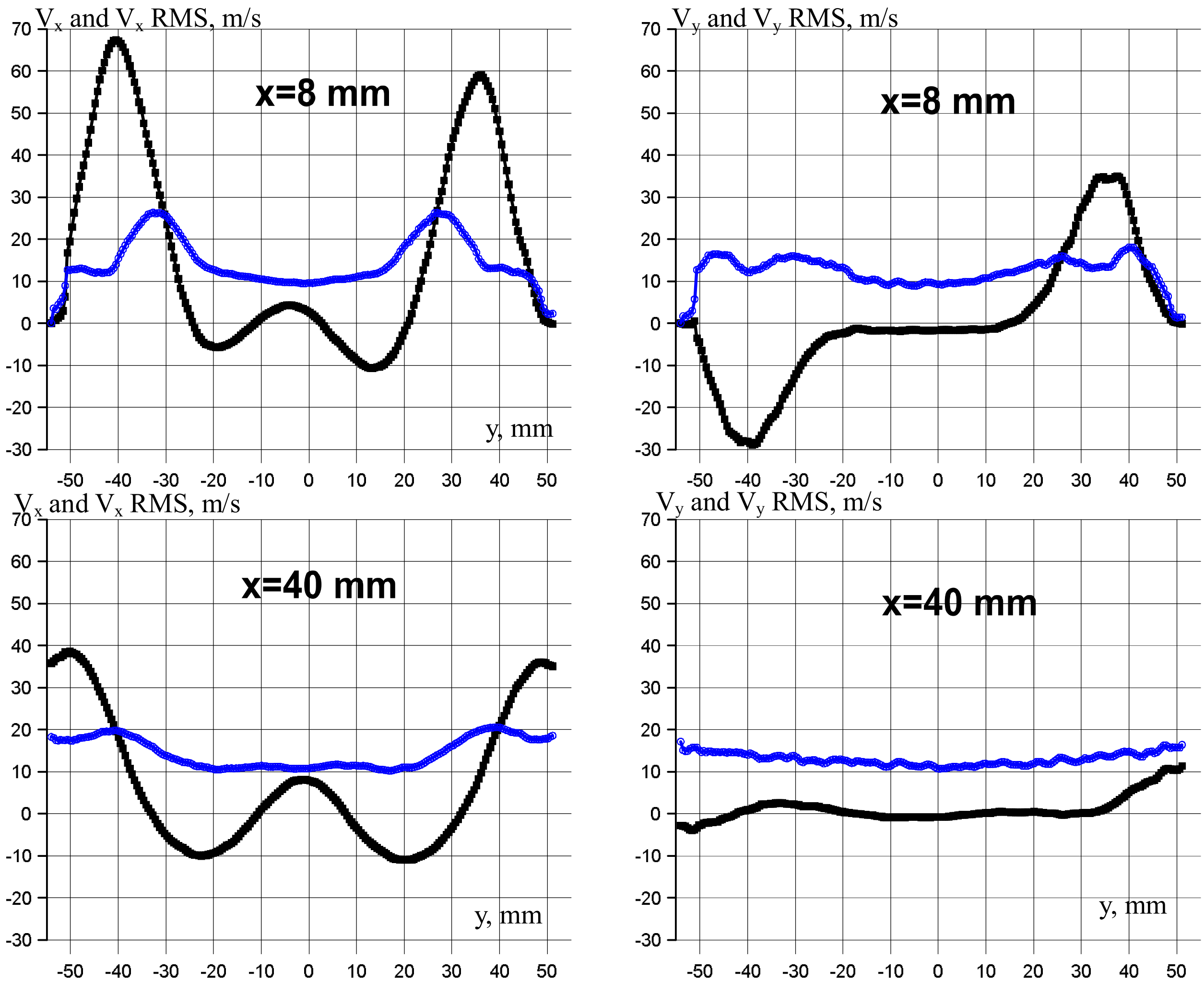

Fig. 6 Radial profiles of the mean (black) and RMS (blue) values of the axial (V_x) and radial (V_y) velocity components

at different distances from the burner

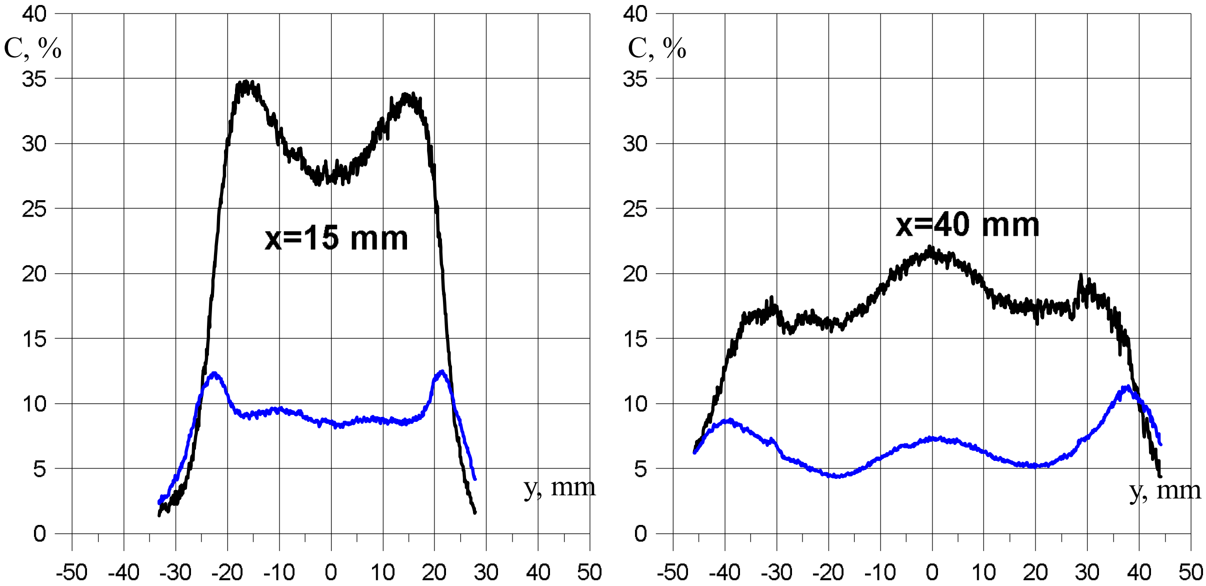

Fig. 7. Mean concentration profiles (black line) and concentration RMS (blue line) at different distances from the burner exit

As can be seen downstream of the nozzle maximum mean concentration decreases 1.6 times. Another feature is that near the burner concentration profile has two well-pronounced maxima. This maxima indicates strong interaction of the central fuel jets with coaxial swirling flow. At the distance of ≈ 0.5D from the burner only one central maxima of concentration is present. The concentration pulsations are quite high near the burner exit (about 30 % of the maximum) and reaches its maximum in the inner shear layer of coaxial swirling flow. Downstream the arbitrary level of concentration pulsations is still about 30 %. The interaction of the flow field and passive admixture concentration field could be clearly seen from the Fig. 8 which illustrates superimposed instantaneous and averaged velocity and concentration measurements results. Instantaneous data shows that maximum concentration gradients are reached in the region of shear layer.

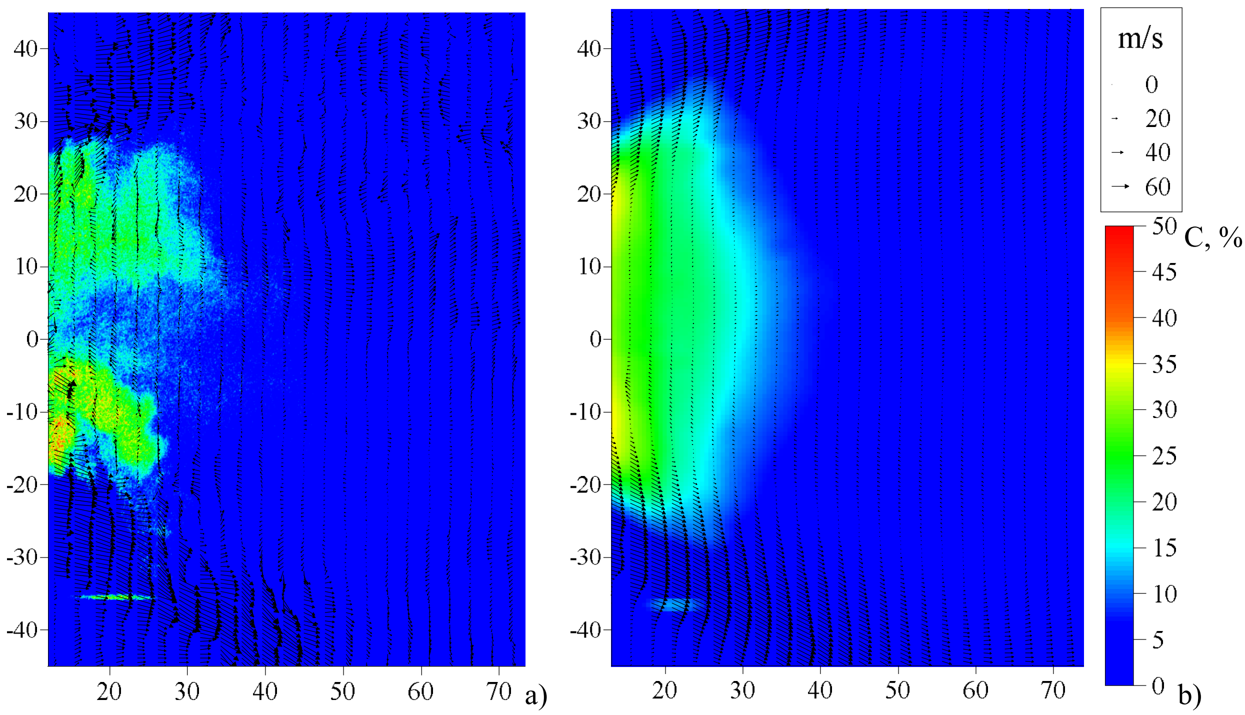

Fig. 8. Instantaneous (a) and averaged (b) velocity field and passive admixture concentration in the central plane of GT combustion chamber (Re=300 000)

Conclusions

In the present work combined PLIF/PIV experiments were carried out in a cold model of GT-burner at realistic flow-rates. The results include instantaneous simultaneously measured 2D concentration of passive admixture and velocity fields. The main goal of the investigation was a better understanding of the turbulent mixing process in an industrial burner and acquisition of experimental data for validation of numerical simulation. Despite of non-perfect quality of quartz glass cylinder and multiple laser sheet reflections data processing algorithms allowed to get reliable experimental data. The results indicates that there is a strong correlation between velocity and concentration fields. The velocity and concentration pulsations reaches its maxima in the shear layers regions. Concentration of the fuel in the central jet decreases slightly downstream the burner, but the concentration in the shear layer between the recirculation zone and main coaxial flow decreases two times at the distance of half burner diameter.

Acknowledgments

This work is funded by a grant from the Russian Science Foundation (project No. 14-29-00203 in NSU, supervised by Professor Kemal Hanjalic).

References

[1] Lozano, A., Smith, S. H., Mungal, M. G., and Hanson, R. K. (1993) Concentration measurements in a trans-verse jet by planar laser-induced fluorescence of acetone *AIAA J.*, vol. 32, pp 218-221.

[2] Su L.K., Mungal M.G. Mixing in cross-flowing jets: Turbulent quantities. In: Proceedings of the 43rd Aerospace Science Meeting and Exhibit 10-13 January, Reno, Nevada, AIAA 2005-305

[3] Raffel M., Willert C., Wereley S., Kompenhans J. (2007) Particle Image Velocimetry. A practical guide, Second Edition, Berlin, Springer.

[4] Bryant RA, Donbar JM, Driscoll JF (2000) Acetone laser induced fluorescence for low pressure/low temperature flow visualization. *Experiments in Fluids* 28(5), pp 471–476. doi: 10.1007/s003480050407, URL http://dx.doi.org/ 10.1007/s003480050407